

DESIGN CONCEPTS FOR A NEXT GENERATION LIGHT SOURCE AT LBNL*

J. N. Corlett[#], A. Allezy, D. Arbelaez, K. Baptiste, J. Byrd, C. Daniels, S. De Santis, W. Delp, P. Denes, R. Donahue, L. Doolittle, P. J. Emma, D. Filippetto, J. Floyd, J. Harkins, G. Huang, J.-Y. Jung, D. Li, T. Pui Lou, T. Luo, G. Marcus, M. T. Monroy, H. Nishimura, H. A. Padmore, C. Papadopoulos, C. Pappas, S. Paret, G. Penn, M. Placidi, S. Prestemon, D. Prosnitz, H. Qian, J. Qiang, A. Ratti, M. Reinsch, D. Robin, F. Sannibale, R. W. Schoenlein, C. Serrano, J. Staples, C. Steier, C. Sun, M. Venturini, W. L. Waldron, W. Wan, T. Warwick, R. Wells, R. Wilcox, S. Zimmermann, M. Zolotarev, LBNL, Berkeley, CA, USA
 C. Ginsburg, R. Kephart, A. L. Klebaner, T. Peterson, A. Sukhanov, FNAL, Batavia, IL, USA
 D. Arenius, G. R. Neil, T. Powers, J. P. Preble, TJNAF, Newport News, VA, USA
 C. Adolphsen, K. Bane, Y. Ding, Z. Huang, C. Nantista, C.-K. Ng, H.-D. Nuhn, C. Rivetta, G. Stupakov, SLAC, Stanford, CA, USA

Abstract

The NGLS collaboration is developing design concepts for a multi-beamline soft x-ray FEL array powered by a superconducting linear accelerator, operating with a high bunch repetition rate of approximately 1 MHz. The CW superconducting linear accelerator design is based on developments of TESLA and ILC technology, and is supplied by an injector based on a high-brightness, high-repetition-rate photocathode electron gun. Electron bunches from the linac are distributed by RF deflecting cavities to the array of independently configurable FEL beamlines with nominal bunch rates of ~100 kHz in each FEL, with uniform pulse spacing, and some FELs capable of operating at the full linac bunch rate. Individual FELs may be configured for different modes of operation, including self-seeded and external-laser-seeded, and each may produce high peak and average brightness x-rays with a flexible pulse format, and with pulse durations ranging from femtoseconds and shorter, to hundreds of femtoseconds. In this paper we describe current design concepts, and progress in R&D activities.

FACILITY OVERVIEW

The NGLS concept is an X-ray free-electron laser array powered by a superconducting accelerator capable of delivering electron bunches to a suite of independently configured FEL beamlines. Each beamline, operating simultaneously at a nominal initial repetition rate of 100 kHz, and with potential for MHz operation in some beamlines, will be optimized for specific science needs.

Figure 1 shows a schematic layout of the proposed facility. Most notable among the design features are a high-repetition-rate (MHz), high-brightness electron source, and a superconducting radio-frequency electron linac operating in CW mode that will provide bunches at high rate, high average beam power, and with uniform bunch spacing. These bunches will be distributed via a spreader system to an array of FELs, and each FEL will

provide average brightness five or more orders of magnitude higher than existing light sources, and two or more orders of magnitude higher than other planned and under construction light sources. Each FEL will be seeded and feature independently adjustable central wavelength, polarization, photon pulse power, and ultrafast temporal resolution, with some beamlines having control of time-bandwidth trade-off. The high average electron beam power allows the capability of up to ~100 W of average X-ray power per beamline. Flux will vary from ~10⁹ to ~10¹² photons per pulse in the fundamental, depending on the wavelength, pulse duration, and FEL design. Figure 2 shows average brightness for self-seeded FELs, covering different photon energy ranges accessible with different electron beam energies.

A 2.4 GeV beam energy configuration has been reported previously [1], in this paper we also briefly outline capabilities for lower and higher electron beam energies, and corresponding photon energy reach, that could be provided by an initial NGLS and its potential upgrades. Each choice of beam energy retains the basic configuration shown in Fig. 1, and the unique technical capabilities of MHz repetition rate of uniformly spaced bunches, femtosecond pulse duration, ~10 meV FEL output bandwidth. The most critical science capabilities are accessed in the K- and L-edges of the earth-abundant elements, as well as diffraction/scattering in the few to several keV photon energy range. The NGLS approach allows flexibility in staging construction, by adjusting the number of cryomodules and FEL beamlines.

NGLS will provide a suite of unique features compared to existing or planned X-ray light sources, and the facility is being designed to expand capabilities in the most critical needs in X-ray science for imaging, structure determination, and spectroscopy. The facility will enable cinematic imaging of dynamics, reveal the structure of heterogenous systems, and allow for development of novel nonlinear X-ray spectroscopies. The uniform pulse spacing at a high repetition rate will provide unprecedented capabilities, accommodating more diverse and challenging experiments than those enabled by current or other planned sources.

*Work supported by the Director, Office of Science, of the U.S. Department of Energy under Contract No. DE-AC02-05CH11231
[#]jncorlett@lbl.gov

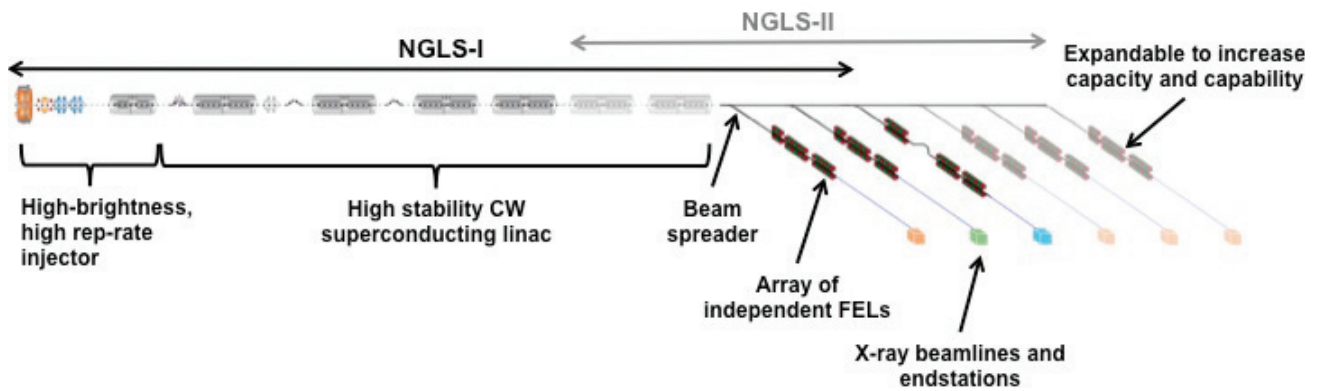


Figure 1: Schematic layout of the main components of NGLS (not to scale), showing the phased approach and major components. NGLS-II would be an upgrade(s) to expand capability and capacity, by increase in beam energy, and/or addition of FELs.

The initial set of three simultaneously operable X-ray FELs will serve a large number of experiments per year, with six end stations (two per FEL). Moreover, the facility's upgrade potential could provide both additional capacity (up to six more FELs) and new capabilities – including, for example, higher photon beam energies, repetition rates, and resolving power; higher average and peak X-ray power; shorter and longer pulses; shorter- and longer-wavelength FELs; additional synchronization and shaping possibilities; and X-ray pulse feedback control.

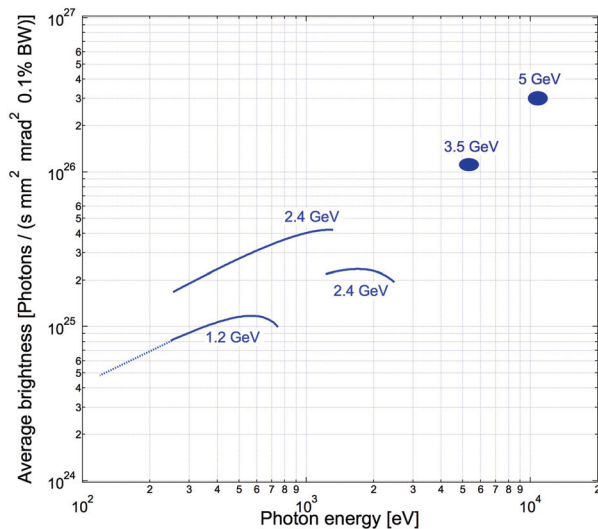


Figure 2: Examples of average brightness of self-seeded FEL configurations, at 1 MHz, as a function of photon energy, for different electron beam energy.

THE MACHINE

The CW superconducting linac will provide a “backbone” for delivering high-brightness and high-repetition-rate electron beams to an array of independent FELs. The machine baseline design concept is for a maximum bunch charge of 300 pC and nominal 1 MHz repetition rate (i.e., an average current of 300 μ A), and with upgrade paths consistent with a range of lower bunch charge at increased rate while maintaining average current. A variety of bunch time structures may be

accommodated by the injector and linac, and our conceptual design allows flexibility to increase versatility in performance. The nominal electron beam energy of 2.4 GeV has been chosen so as to be able to produce tunable FELs which together cover an operating range from 100 eV and up to 1.2 keV photon energy in the fundamental, and 6 keV and beyond in harmonics. An alternate, low cost configuration with a 1.2 GeV linac has also been studied, which could produce a photon energy range of 50 – 720 eV in the fundamental – still accessing the K- and L-edges of the most abundant elements. Upgrade options include adding cryomodules to the main linac to increase beam energy, and a 3.5 GeV linac could extend the X-ray reach to 5 keV in the fundamental (with limited tuning range), and higher electron beam energies providing harder X-rays (5 GeV reaches the 10 keV range). For the highest energies additional cryomodules may be placed in a spreader arm dedicated to the hardest X-ray FELs, with soft X-ray capabilities provided by the better-matched lower energy beam. Linac length is approximately 210 m for 1.2 GeV, 340 m for 2.4 GeV, 460 m for 3.5 GeV, 610 m for 5 GeV.

Injector

The photoinjector is designed to operate at 1 MHz repetition rate and deliver the nominal 300 pC bunch charge, although up to 1 nC pulse charge may be possible, and higher repetition rate but at correspondingly lower charge. The electron beam is produced at a high quantum efficiency photocathode installed at the end of a re-entrant nosecone mounted in a 186 MHz normal conducting copper cavity operating in CW mode. A drive laser using commercially available technology illuminates the photocathode, and a “bucking” solenoid integrated into the nosecone of the gun controls the magnetic field at the cathode surface. Following the gun are a solenoid, followed by a buncher cavity, and then a second solenoid. These elements initiate emittance compensation and “ballistic” bunch compression. Then follows an accelerating cryomodule containing eight 1.3 GHz CW TESLA-like superconducting 9-cell cavities. Each cavity has independent control of accelerating field phase and

amplitude. This cryomodule, identical to the main linac cryomodules (although possibly with a re-design of the power coupler for the initial cavities to minimize transverse kicks to the low-energy beam), accelerates the beam from 750 keV at the gun exit and performs velocity bunching by de-phasing the RF with respect to the maximum acceleration phase in the initial cavities. The injector is designed to deliver bunches with 30-50 A peak current, slice energy spread ≤ 15 keV, and normalized emittance ≤ 0.6 mm-mrad, at about 95 MeV [2,3].

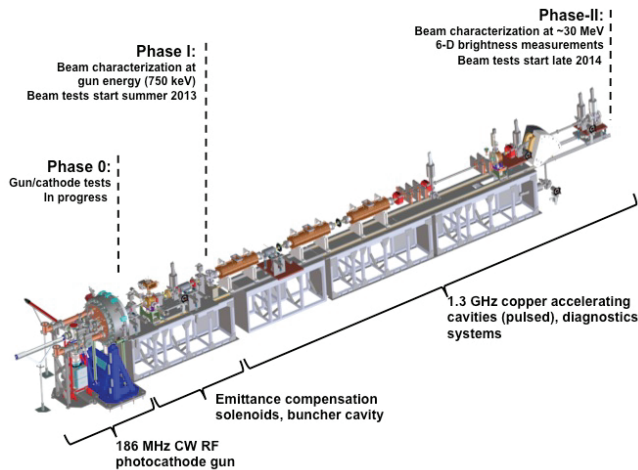


Figure 3: Schematic of the APEX R&D project to demonstrate and test high repetition rate high-brightness electron injector technology for future light sources.

An R&D project, called ‘‘APEX’’, is under way at LBNL to prototype an injector suitable for the NGLS. Figure 3 shows a schematic of the APEX injector and phases of the project. Pulsed normal conducting accelerating structures will be used as a cost-effective means for the proof-of-principle demonstration.

Fabrication of components through Phase-I is complete, and beam characterization will begin in summer 2013. The gun technology has been demonstrated at full RF power (producing ~ 20 MVm⁻¹ at the cathode) and with MHz rate photo-emitted electron bunches extracted from a Cs₂Te cathode, while maintaining excellent vacuum ($\sim 10^{-10}$ Torr with RF power, base pressure $\sim 10^{-12}$ Torr). Lifetime and dark current measurements have begun, details may be found in [4,5].

Linac

Choices for beam energy and pulse repetition rates are motivated by the science needs for X-ray laser pulses, and FEL technology, and necessitate the adoption of CW SCRF technology for the linac. The linac will accept electron bunches from the injector, provide acceleration and bunch compression, before directing the beam to the spreader for distribution into the separate FEL undulator lines. The linac, based on the choice of existing 1.3 GHz TESLA-like superconducting cavity technology, will consist of seven main sections, as indicated in Fig. 4. The first section, the laser heater, will interface the linac with the injector, and provide control of the beam energy spread and stabilize the longitudinal beam dynamics. The

beam will then be accelerated in Linac 1, conditioned by passage through a 3.9 GHz RF structure to linearize the correlated energy spread, compressed through a single-chicane bunch compressor, and then further accelerated in Linac 2. A second bunch compressor would allow for further manipulations of the longitudinal phase space, and the final energy would be achieved in Linac 3, the last linac section. Given the 30-50 A range for the peak current out of the injector, a 10-17 compression factor is required in the linac in order to deliver ~ 500 A peak current to the FELs, in a usable section of beam of up to ~ 300 fs. The longitudinal wakefield in the linac is not sufficient to completely remove the energy chirp after bunch compression, and to accomplish this a ‘‘de-chirper’’ section of narrow-aperture passive insertions with enhanced longitudinal wakefield is planned to follow the main linac [6,7]. Beam dynamics studies are further described in [8,9].

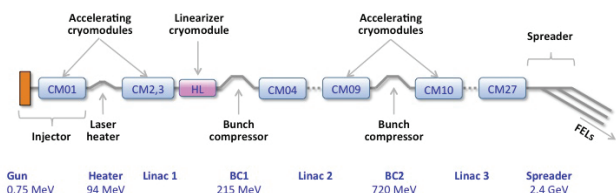


Figure 4: Schematic of the major accelerator components, for the baseline 2.4 GeV configuration.

Based on the ILC technology, and with developments for CW operation, the NGLS linac will feature discrete cryomodules each with cold/warm transitions, 8 RF cavities per cryomodule, and with magnets, diagnostics & higher-order-mode (HOM) absorbers located in warm beampipe sections between cryomodules. Studies of HOM effects show only small amounts of power dissipated in cavities from resonant HOMs or from modes above cut-off, and no significant impact on beam dynamics. Typical dynamic losses will be ~ 12 W per cavity, assuming a Q_0 of 2×10^{10} at 1.8 K, and average operating gradient of 14 MVm⁻¹. Installed RF power will be ~ 6 kW per cavity, assuming a detuning of ± 15 Hz and Q_{ext} of 3.1×10^7 . The cryogenics systems will distribute 5 K liquid, cooled to 1.8 K by expansion at each cryomodule. The cryoplant will be designed for He mass flow similar to an existing LHC cryoplant also operating at 1.8 K. Figure 5 shows an engineering layout of a cryomodule. Figure 6 shows a schematic of the cryogenics distribution circuits.

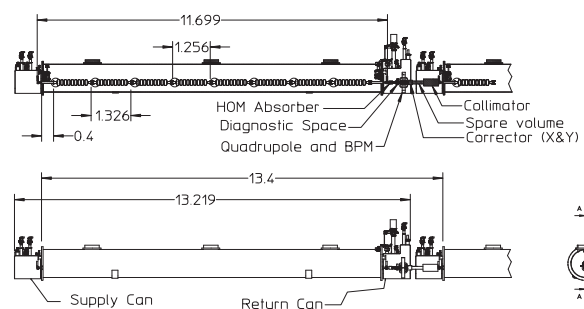


Figure 5: Cryomodule layout (dimensions in m).

In addition to supporting the required high repetition rate, a CW superconducting linac provides excellent beam stability. Further discussion of the linac design can be found in [10, 11, 12, 13].

The accelerator and support systems will be housed in separate tunnels, with connections for RF waveguide distribution and power supplies and signals (Figure 7). This allows for access to equipment in the support tunnel, while the accelerator is operating.

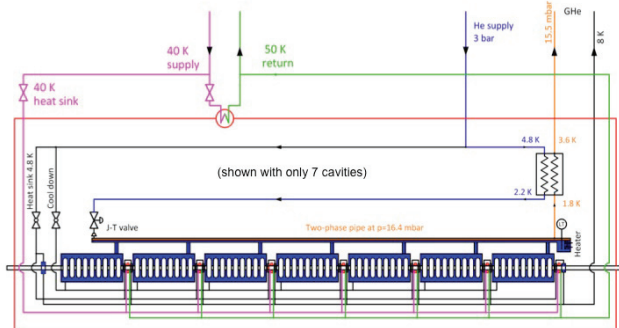


Figure 6: Schematic of the cryogenics distribution circuits.

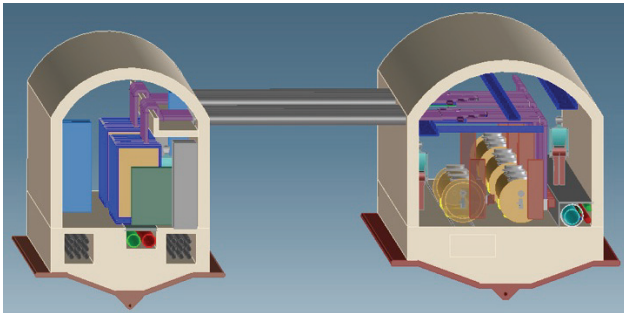


Figure 7: NGLS tunnel configuration, showing a support and services tunnel on the left and the accelerator housing on the right. An additional cryomodule is shown to indicate the space available for installation.

Spreader

The spreader is designed to deliver individual bunches to the array of FELs, using a series of deflecting radio frequency cavities and electron beam transport lines. The scheme adopts superconducting RF dipole cavities [14] that provide a vertical deflection for bunches arriving at the RF waveform maxima (\pm), and a straight-through path at the zero-crossing (see Figure 8 for a schematic layout). The emerging trajectories are then deflected by a Lambertson septum magnet or a dipole to create a three-way horizontal distribution.

Vertical offsets are corrected in the downstream beam transport. Following each of the initial beam “take-off” sections is a transport section consisting of two triple-bend achromats providing achromatic and isochronous properties up to the FEL entrance. The beamlines have a 36-deg total deflection to optimize beam optics properties within a reasonable footprint and provide ~ 5.5 m separation between the undulator lines [15, 16]. The process may be repeated to produce additional beamlines in groups of three (and potentially other arrangements).

ISBN 978-3-95450-126-7

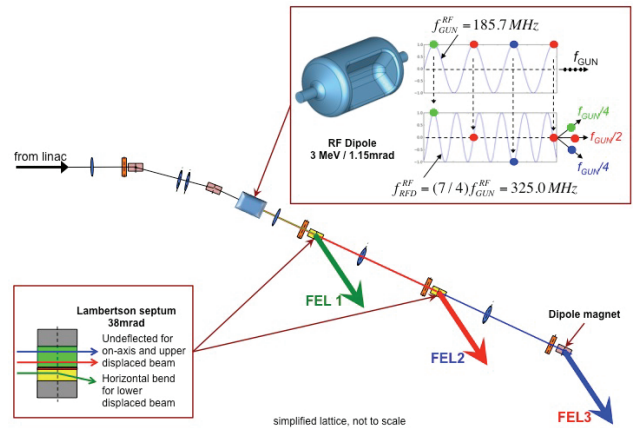


Figure 8: Simplified schematic diagram of the beam spreader.

Collimation

NGLS will employ a distributed collimation system [17]. In the injector, in addition to general collimation of large transverse amplitude particles, a dark current kicker will clear out most of the dark current buckets without perturbing the main bunches. The next stage consists of multiple energy collimators, located in the middle of each of the bunch compressors as well as in the laser heater chicane to reduce beam losses in the superconducting linac and achieve collimation at the lowest beam energy feasible. The post-linac collimation removes the beam halo particles in a transverse collimation section with approximately 90-degree phase advance between each set of horizontal and vertical collimators. Finally there is another energy collimation section that makes use of the dispersion at the beginning of each of the spreader arcs. The geometry of the spreader prevents particle showers generated by the collimators from entering the undulator sections.

Superconducting Undulators

Superconducting undulators offer significant performance enhancement over conventional hybrid-permanent-magnet devices: larger tuning range at a given beam energy, maintaining tuning range at a lower beam energy, shorter undulator array, and radiation resistance.

To optimize performance of the NGLS, the FELs are designed using Nb₃Sn undulator technology. A 0.5 m long, 20 mm period, 7.5 mm magnetic gap, 2T peak on-axis field, Nb₃Sn prototype device is under construction at LBNL, with initial results expected in fall 2013. A cryostat and magnet measurement system has been built for tests, and techniques for field trimming using superconducting trim coils will be developed and tested [18]. Figure 9 shows a comparison of different undulator types, with examples of each indicated. A superconducting NbTi undulator has been successfully installed and operated at the Advanced Photon Source [19], and this or hybrid-permanent-magnet technology could also be used if this should prove advantageous. Wakefield effects in the undulators have an important

impact of FEL performance, and recent developments in understanding are reported in [20,21].

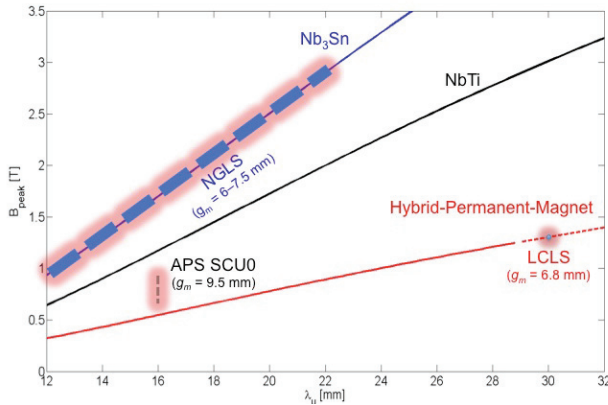


Figure 9: Comparison of undulator technologies, showing higher peak field achievable with superconducting devices of a given period. The lines are for a 7.5 mm gap, with examples shown for each technology (at labelled magnetic gap). For NGLS, period and gap would be determined by electron and photon beam energy requirements, and vary between each FEL beamline.

FELs

The NGLS design incorporates multiple FEL beamlines, and the initial array of 3 independent X-ray FELs will use seeding techniques to impart temporal coherence approaching fundamental transform limits.

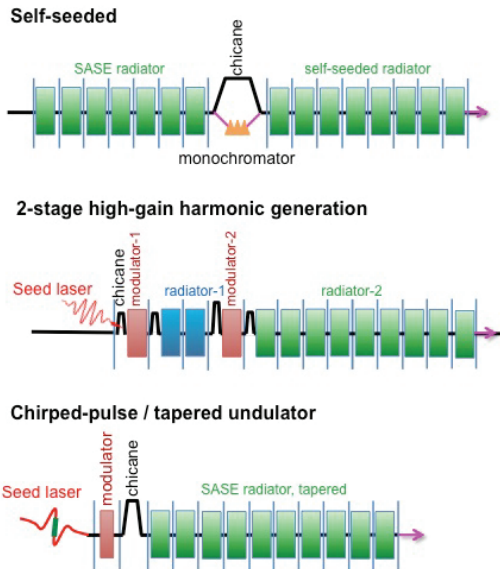


Figure 10: Three nominal initial seeded FEL concepts.

Three FEL concepts are currently being developed, as shown in Figure 10 [22,23,24]. The first, soft X-ray self-seeding (SXRSS), is independent of external laser technology and may provide the highest average power beams. The second, high-gain harmonic generation (HGHH), benefits from recent successes at FERMI@elettra [25]. The third produces intense ultrafast pulses using a few-cycle seed laser pulse to energy chirp the electron beam, and tapered undulator to compensate

for gain degradation within the chirped part of the pulse – outside this region gain is suppressed [22,26]. Other FEL configurations such as EEHG may also be implemented at NGLS, and are a continued subject of R&D studies [27].

After successful demonstration of hard X-ray self-seeding at the LCLS [28], a multi-laboratory collaboration is now extending the capability to soft x-rays. Figure 11 shows the arrangement of the monochromator and electron beam delay line, designed and fabricated by a collaboration between LBNL, SLAC, and PSI. The SXRSS project aims to provide resolving power of at least 5000 across the photon energy range of 500-1000 eV, and is planned to be installed in the LCLS in 2013 [29].

For NGLS, we anticipate higher resolving power of 20,000, and average brightness exceeding 10^{25} ph/s/mm²/mrad²/0.1%BW in the soft X-ray range, and higher at 5 keV and greater (see Fig.2). Self-seeding will allow operation with the full electron beam from the linac, with up to ~100 W coherent X-ray power, in an FEL ~100 m long or less (including breaks and diagnostics).

Laser seeding will be implemented in some beamlines to produce pulses with duration as short as ~1 fs (and potentially less in some configurations), with (1) temporal coherence approaching fundamental transform limits, (2) the possibility of using the chirp in photon pulse output for further compression in X-ray optics, and (3) synchronization of the X-ray pulses and timing with respect to end-station lasers with ≤10 fs precision. The HGHH approach allows trade-off of time and bandwidth, approaching Fourier-transform limits, and narrow bandwidth out of the FEL in the few to several tens of meV range. Laser seeding reduces the length of the FEL compared to self-seeding, and a two-stage HGHH configuration reaching a photon energy of 600 eV, and with 10^{11} – 10^{12} ph/pulse in the fundamental is ~60 m long. A chirped-pulse tapered undulator scheme of ~60 m length has been developed that produces up to 10^9 – 10^{10} ph in a pulse ~1 fs long.

Seed laser systems require ~200 MW peak power in the UV for the HGHH FEL, and ~5 GW peak power in a few-cycle 2.1 μm carrier-envelope stabilized source for the chirped pulse approach. A concept for the HGHH laser is shown in Figure 12, further details on seed lasers may be found in [30].

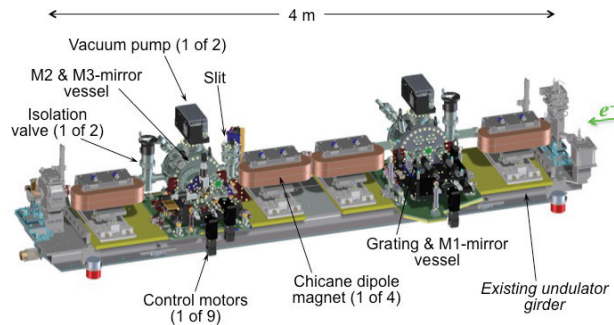


Figure 11: SXRSS hardware under construction for test at the LCLS.

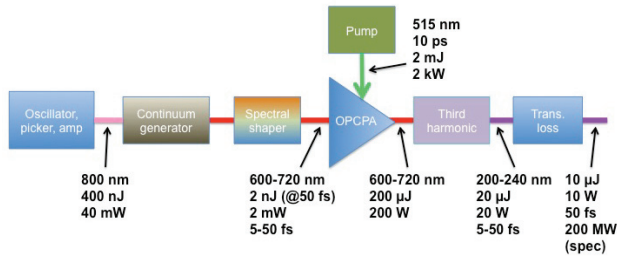


Figure 12: UV seed laser concept for HGHG, allowing up to MHz repetition rate for ~ 50 fs pulses (and lower repetition rate for higher per-pulse energy).

Two-color Capability

“Two-color” X-ray pulse capability may be provided by synchronizing two independent FELs, or by seeding different parts of a single electron bunch which is passed through two separate FELs. Either approach allows coverage of the full tuning range of each FEL, with timing variations up to picoseconds. Figure 13 shows a configuration with FELs in separate spreader beamlines. The difference in bunch travel times ($A \rightarrow B$) – ($A \rightarrow C$) will be made equal to the bunch spacing at the photocathode gun, by design of the magnetic lattice. Additional timing adjustment will be provided by a chicane shown in arm ($A \rightarrow C$), which provides ± 600 fs variation in electron beam arrival time at the FEL. Seed laser timing provides fine control, and X-ray optics provide further timing delay up to picoseconds. Figure 14 shows a different approach, generating ultrafast two-color pulses by seeding different parts of a single electron bunch which is passed through two sequential chirped-pulse / tapered undulator FELs (as discussed in the previous section).

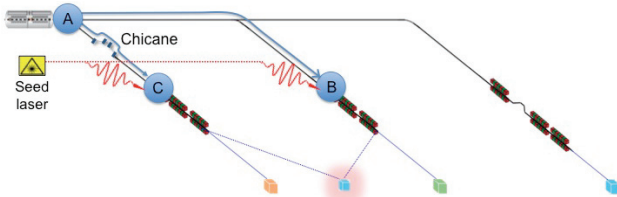


Figure 13: Schematic of two-color capability obtained by delivering synchronized and adjustable output from two independent FELs to a single endstation, see text for explanation.

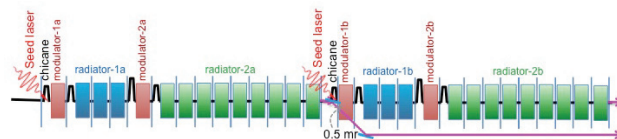


Figure 14: Schematic of a second approach to two-color capability, generating pulses by seeding different parts of a single electron bunch which is passed through two separate chirped-pulse / tapered undulator FELs. The X-ray beam from the first FEL is separated by optics and propagates a few mm apart from the beam through the second FEL.

ISBN 978-3-95450-126-7

Pulse-on-demand

Single-particle-imaging has been a goal of FEL-based science [31], and the development of sample injectors has progressed significantly [32]. The most important limitation for single-particle-imaging is the low hit rate. Pulse-on-demand is a unique feature of the NGLS that will enable a significant increase in hit rate. Detection with photodiodes measures timing and predicts the path of a particle emerging from the injector. The NGLS photocathode is then triggered to provide an FEL pulse coincident with the particle arrival at the FEL focus. The concept is shown schematically in Figure 15.

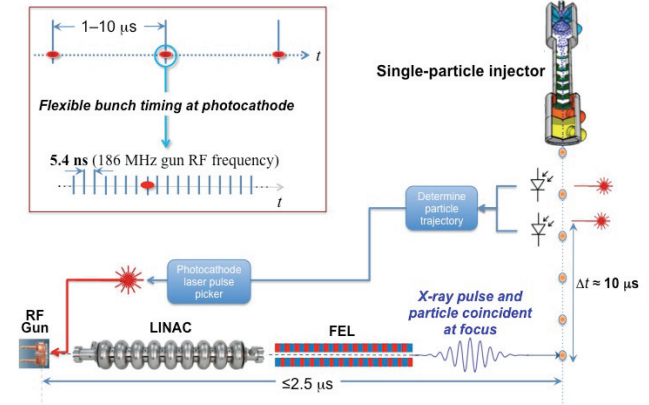


Figure 15: Schematic of the pulse-on-demand technique. The CW RF systems and flexible photocathode gun laser timing allow selection of bunch timing to produce an X-ray pulse coincident with a particle.

ACKNOWLEDGEMENTS

The authors thank Dr. J. Spence and Dr. U. Weierstall for helpful discussions on sample injectors and pulse-on-demand techniques at FELs.

REFERENCES

- [1] J.N. Corlett et al., “Next Generation Light Source R&D and design studies at LBNL” Proc IPAC2012, New Orleans, Louisiana, USA, May 20-25, 2012 TUPP070
- [2] C.F. Papadopoulos et al., “Injector beam dynamics for a 4th generation light source” Proc IPAC2012, New Orleans, Louisiana, USA, May 20-25, 2012 WEPPO31
- [3] C.F. Papadopoulos et al., “Injector Design Studies for NGLS”, Proceedings of the 2013 FEL Conference, New York, USA (2013).
- [4] F. Sannibale, et al., “Advanced photoinjector experiment photogun commissioning results” PRST-AB **15**, 103501 (2012)
- [5] D. Filippetto et al., “The Photocathode Laser System for the APEX High Repetition Rate Photoinjector”, Proceedings of the 2013 FEL Conference, New York, USA (2013).
- [6] K. Bane and G. Stupakov, “Corrugated pipe as a beam dechirper” Nucl. Instr. and Methods A, **690**, 106-110 (2012).

- [7] H.-S. Kang, “Control of Electron Beam Longitudinal Phase Space with a Novel Compact De-chirper”, Proceedings of the 2013 FEL Conference, New York, USA (2013).
- [8] M. Venturini et al., “Beam Dynamics Studies of a High-repetition Rate Linac-Driver for 4th Generation Light Source”, IPAC2012, New Orleans, Louisiana, USA, May 20-25, 2012, TUPPP074.
- [9] J. Qiang et al., “Start-to-end simulation of a Next Generation Light Source using the real number of electrons”, Proceedings of the 2013 FEL Conference, New York, USA (2013).
- [10] J. Corlett et al., “Superconducting linac design concepts for a Next Generation Light Source at LBNL”, Proceedings of the 2013 FEL Conference, New York, USA (2013).
- [11] A. Ratti et al., “RF Design of the NGLS Linac”, Proceedings of the 2013 FEL Conference, New York, USA (2013).
- [12] J. Byrd et al., “Towards high energy and timing stability in SCRF linacs”, Proceedings of the 2013 FEL Conference, New York, USA (2013).
- [13] S. DeSantis et al., “Beam Diagnostic Requirements for the Next Generation Light Source”, Proceedings of the 2013 FEL Conference, New York, USA (2013).
- [14] S. U. De Silva & J. R. Delayen “Design evolution and properties of superconducting parallel-bar rf-dipole deflecting and crabbing cavities” PRST-AB **16**, 012004 (2013)
- [15] M. Placidi et al., “Design Concept of a Deflection Cavity Based Spreader System for a Next Generation Free Electron Laser”, Proc. IPAC’13, Shanghai China, May 12-17 2013 WEPWA069
- [16] C. Sun et al., “Design concept of an RF-based beam-spreader system for a Next Generation Light Source”, Proceedings of the 2013 FEL Conference, New York, USA (2013).
- [17] C. Steier et al., “Design of a Collimation System for the Next Generation Light Source”, Proceedings of the 2013 FEL Conference, New York, USA (2013).
- [18] E. Rochepault et al., “Error Analysis and Field Correction Methods in Superconducting Undulators”, Proceedings of the 2013 International Conference on Magnet Technology, Boston, USA (2013).
- [19] <http://www.aps.anl.gov/Upgrade/News/first-light.html>
- [20] G. Stupakov and S. Reiche, “Surface roughness wakefield in FEL undulator”, Proceedings of the 2013 FEL Conference, New York, USA (2013).
- [21] Ji Qiang, Chad Mitchell, “Suppression of Wakefield Induced Energy Spread Inside an Undulator Through Current Shaping”, Proceedings of the 2013 FEL Conference, New York, USA (2013).
- [22] G. Penn et al., “Three Unique FEL Designs for the Next Generation Light Source” Proceedings of the 2013 FEL Conference, New York, USA (2013).
- [23] G. Penn et al., “Simulation Studies Of FELs For A Next Generation Light Source”, Proceedings of the 2013 FEL Conference, New York, USA (2013).
- [24] M. Reinsch et al., “FEL X-ray Pulse Brightness Calculations”, Proceedings of the 2013 FEL Conference, New York, USA (2013).
- [25] <http://www.elettra.trieste.it/lightsources/fermi.html>
- [26] L. Gianessi et al., “Self-Amplified Spontaneous Emission Free-Electron Laser with an Energy-Chirped Electron Beam and Undulator Tapering” PRL **106**, 144801 (2011)
- [27] G. Stupakov, “Effect of coulomb collisions on echo-enabled harmonic generation”, Proceedings of the 2013 FEL Conference, New York, USA (2013).
- [28] J. Amman et al, “Demonstration of self-seeding in a hard-X-ray free-electron laser” Nature Photonics **6**, 693–698 (2012)
- [29] D. Ratner et al., “Soft X-ray Self Seeding Project at LCLS”, Proceedings of the 2013 FEL Conference, New York, USA (2013).
- [30] R. Wilcox et al., “High average power seed laser design for high repute FELs”, Proceedings of the 2013 FEL Conference, New York, USA (2013).
- [31] M. Siebert et al., “Single mimivirus particles intercepted and imaged with an X-ray laser” Nature **470**, 78–81 (February 2011)
- [32] U. Weierstall et al., “Injector for scattering measurements on fully solvated biospecies” Rev SciInstrum **83**, 035108 (2012)